

Spontaneous bone metastases in a preclinical orthotopic model of invasive lobular carcinoma; the effect of pharmacological targeting TGF β receptor I kinase

Jeroen T Buijs,^{1*} Kasia M Matula,¹ Henry Cheung,¹ Marianna Kruithof-de Julio,^{2,3} Maaïke H van der Mark,¹ Thomas J Snoeks,⁴ Ron Cohen,¹ Willem E Corver,⁵ Khalid S Mohammad,⁶ Jos Jonkers,⁷ Theresa A Guise⁶ and Gabri van der Pluijm¹

¹ Department of Urology, Leiden University Medical Centre, Leiden, The Netherlands

² Department of Molecular Cell Biology, Leiden University Medical Centre, Leiden, The Netherlands

³ Department of Dermatology, Leiden University Medical Centre, Leiden, The Netherlands

⁴ Department of Radiology, Leiden University Medical Centre, Leiden, The Netherlands

⁵ Department of Pathology, Leiden University Medical Centre, Leiden, The Netherlands

⁶ Department of Medicine, Division of Endocrinology, Indiana University School of Medicine, Indianapolis, IN, USA

⁷ Division of Molecular Pathology, Netherlands Cancer Institute, Amsterdam, The Netherlands

*Correspondence to: Jeroen T Buijs, Department of Urology, Leiden University Medical Centre, J3-64 Albinusdreef 2, 2333 ZA Leiden, The Netherlands. e-mail: J.T.Buijs@LUMC.nl

Abstract

Invasive ductal carcinoma (IDC) and invasive lobular carcinoma (ILC) are the most frequently occurring histological subtypes of breast cancer, accounting for 80–90% and 10–15% of the total cases, respectively. At the time of diagnosis and surgical resection of the primary tumour, most patients do not have clinical signs of metastases, but bone micrometastases may already be present. Our aim was to develop a novel preclinical ILC model of spontaneous bone micrometastasis. We used murine invasive lobular breast carcinoma cells (KEP) that were generated by targeted deletion of E-cadherin and p53 in a conditional *K14cre;Cdh1^(F/F);Trp53^(F/F)* mouse model of *de novo* mammary tumour formation. After surgical resection of the growing orthotopically implanted KEP cells, distant metastases were formed. In contrast to other orthotopic breast cancer models, KEP cells readily formed skeletal metastases with minimal lung involvement. Continuous treatment with SD-208 (60 mg/kg per day), an orally available TGF β receptor I kinase inhibitor, increased the tumour growth at the primary site and increased the number of distant metastases. Furthermore, when SD-208 treatment was started after surgical resection of the orthotopic tumour, increased bone colonisation was also observed (versus vehicle). Both our *in vitro* and *in vivo* data show that SD-208 treatment reduced TGF β signalling, inhibited apoptosis, and increased proliferation. In conclusion, we have demonstrated that orthotopic implantation of murine ILC cells represent a new breast cancer model of minimal residual disease *in vivo*, which comprises key steps of the metastatic cascade. The cancer cells are sensitive to the anti-tumour effects of TGF β . Our *in vivo* model is ideally suited for functional studies and evaluation of new pharmacological intervention strategies that may target one or more steps along the metastatic cascade of events.

© 2014 The Authors. *The Journal of Pathology* published by John Wiley & Sons Ltd on behalf of Pathological Society of Great Britain and Ireland.

Keywords: mouse model; metastasis; minimal residual disease; TGF β ; SD-208; receptor I kinase inhibitor; breast cancer; invasive lobular carcinoma

Received 21 July 2014; Revised 14 November 2014; Accepted 21 November 2014

No conflicts of interest were declared.

Introduction

Breast cancer is the most common malignancy among females in the Western world, affecting 12% of the female population. Invasive ductal carcinoma (IDC) and invasive lobular carcinoma (ILC) are the most frequently occurring histological subtypes of breast cancer, accounting for 80–90% and 10–15% of the total cases, respectively [1,2]. For both subtypes, bone is the preferred site of metastasis, leading to incurable and painful disease [3].

Although at the time of diagnosis most breast cancer patients may not have clinical pathological signs of metastases, micrometastases are often present, representing a disease stage called ‘minimal residual disease’ (MRD). The micrometastases may stay dormant for many years before developing into clinically overt metastases. Hence, there is an urgent need for a preclinical *in vivo* model that mimics these key events during breast cancer progression. Such preclinical models will facilitate the development of a novel treatment for advanced breast cancer aiming at improving

clinical outcome. Unfortunately, most of the currently available *in vivo* bone metastasis models do not reflect the complex, multistep process of metastasis [4,5]. For example, models that rely on intra-arterial inoculation of cancer cells only represent later stages of metastasis, i.e. tumour cell extravasation, and homing to distant sites.

Genetically engineered mouse models (GEMMs) of *de novo* tumourigenesis and subsequent metastasis formation offer several advantages. Tumours derived from GEMMs often closely recapitulate the histopathological characteristics observed in clinical material. Moreover, tissue-specific induction of mutations gives rise to orthotopic tumours in the context of a functional, competent microenvironment, thus recapitulating the crosstalk between the tumour and its stroma. Unfortunately, GEMMs often yield a relatively low incidence of metastatic disease [6]. Direct inoculation of cancer cells into the mammary fat pad of mice generally results in tumour take in an anticipated time frame, while still carefully reflecting cancer cell intrinsic traits of the carcinomas.

Most orthotopic models of breast cancer, however, do not result in multiple, detectable metastases to bones. In the highly aggressive, E-cadherin-expressing 4T1 triple-negative murine breast cancer model, small skeletal metastases only occur at late stage, while these mice have suffered from multiple, debilitating lung metastases and invasively growing orthotopic cancer cells [7–9]. In this study, we set out to develop a novel, clinically relevant mouse model of MRD for ILC by exploiting a cell line derived from the well-characterized conditional *K14cre;Cdh1^{F/F};Trp53^{F/F}* mouse model of *de novo* mammary tumour formation [10].

Transforming growth factor- β (TGF β) plays an essential role in maintaining physiological epithelial homeostasis in many tissues through its ability to induce cell cycle arrest, differentiation, and apoptosis, thereby preventing uncontrolled proliferation [11,12]. However, in tumour progression, cancer cells often become refractory to this growth inhibition, and pro-tumourigenic actions of TGF β may prevail, including immunosuppression, angiogenesis, and acquisition of an invasive phenotype [11,12]. In many preclinical breast cancer models, pharmacological inhibition of TGF β signalling was found to reduce metastasis to lung and bone in GEMMs and xenograft mouse models [13–17]. Therefore, many drugs that target the TGF β pathway have been developed, some of which are currently being tested in clinical trials [13,18]. However, the effects of blocking TGF β signalling have not yet been studied in preclinical models of ILC.

Materials and methods

Cell line and culture conditions

The murine invasive lobular carcinoma cell line (KEP) was generated by targeted deletion of E-cadherin and

p53 in a conditional *K14cre;Cdh1^{F/F};Trp53^{F/F}* mouse model as described previously [10]. The lentivirally luciferase transduced clones KEP1_11/Luc (KEP11/Luc) and KEP1_23/Luc (KEP23/Luc) were cultured in DMEM-F12 supplemented with 10% FCS, 50 IU/ml penicillin, 50 ng/ml streptomycin, 5 ng/ml insulin, and 5 ng/ml EGF (Sigma-Aldrich, Zwijndrecht, The Netherlands). Cell lines were tested for *Mycoplasma* contamination by PCR prior to use.

Luciferase reporter gene constructs

The *CAGA*₁₂ reporter construct consists of 12 Smad3/Smad4 binding sequences (CAGA boxes) [19] and was coupled to a *Renilla* luciferase to detect intracellular Smad3/4-dependent TGF β signalling.

DNA staining for cell cycle analysis

KEP cells were seeded (100 000 in T25) and stimulated the subsequent day with TGF β 1 (R&D Systems, Abingdon, UK) and/or SD-208 (Epichem Pty Ltd, Murdoch University, Australia), a small molecule that blocks ATP binding to the TGF β receptor I (T β RI) to specifically inhibit its kinase activity [20]. Cells cultured for 72 h in serum-deprived media were used as positive controls for increase in G0/1. After 24 or 48 h of stimulation, cells were washed twice with PBS and harvested using 0.1% trypsin/EDTA solution, and 300 000 cells were used for staining. Cells were fixed in 80% ethanol and stored at -20°C overnight. Fixed cells were washed in PBS and incubated for 30 min at room temperature in 50 $\mu\text{g/ml}$ RNaseA and 50 $\mu\text{g/ml}$ propidium iodide (PI) solutions, and then placed on ice until analysis. An LSRII flow cytometer (BD Biosciences, San José, CA, USA) supplied with FACSDiva software was used for acquisition. A Sapphire 488 nm, 20 mW laser (Coherent, Santa Clara, CA) was used for excitation of PI and fluorescence was collected using a 610/20 nm band-pass filter. Using the PI pulse-width versus PI pulse-area signals, a life gate was set during acquisition allowing the collection of 40 000 single cell events. A data file contained all events including debris and clumps. The voltage of the PI detector was adjusted to set the mean of the G0/G1 population at channel 50 000. The data were analysed using WinList 7.1 and Modfit 3.3. software packages (Verity Software House, Inc, Topsham, ME, USA) and reports were generated automatically. The S-phase was calculated using the polynomial model, which gave the best fit of the data as calculated by a reduced chi-squared test (<3%). The coefficient of variation (CV) of the G0/1 population never exceeded 4%, demonstrating the high quality of the generated DNA histograms.

Transwell invasion assay

Invasion assays were performed using 24-well transwells (8 μm pore size; Corning B.V. Life Sciences, Amsterdam, The Netherlands). After starving the cells in 0.2% FCS overnight, 40 000 cells were seeded in the

upper chambers of the wells in 0.2% FCS, while the FCS concentration in the lower chamber was 10%.

Twenty-four hours after adding appropriate concentrations of TGF β 1 and SD-208 to both chambers, cells on the filter were fixed with 4% paraformaldehyde and stained with 0.5% crystal violet. Cells in at least three random microscopic fields (20 \times) per membrane were counted.

Animals

Female athymic nude mice (Balb/c *nu/nu*) were purchased from Charles River (L'Arbresle, France) and housed in individual ventilated cages under sterile conditions; sterile food and water were provided *ad libitum*. Animal experiments were approved by the local committee for animal health, ethics, and research of Leiden University and carried out in accordance with European Communities Council Directive 86/609/EEC. After the experimental periods, mice were anaesthetised and sacrificed by cervical dislocation. Tumours were dissected and processed for further histomorphometrical analysis as described earlier [21].

Animal models

Tumour cells were harvested at 70–80% confluence and immediately stored on ice before inoculation *in vivo*. In the intracardiac inoculation model, mice were anaesthetised with an induction dose of 3% isoflurane and maintained under anaesthesia at a dose of 1% isoflurane. In the intra-osseous inoculation model and the surgical resection of the orthotopic tumour, mice were anaesthetised with an induction dose of 3% isoflurane and maintained under anaesthesia at a dose of 2–3% isoflurane.

In the intracardiac inoculation model, a single-cell suspension of 10⁵ cells/100 μ l of PBS was injected into the left cardiac ventricle in isoflurane-anaesthetised 6-week-old mice using a 30-gauge needle (30G 1/2, BDMicro-Fine; Becton Dickinson, Etten-Leur, The Netherlands) [22]. In the intra-osseous inoculation model, a single-cell suspension of 10⁵ cells/100 μ l of PBS was injected into the right tibia of 7-week-old mice [23]. Tibiae were sutured with stainless steel autoclips (Leica Biosystems, Nussloch, Germany), which were gently removed 1 week later.

In the orthotopic model, the fourth inguinal mammary pad of non-anaesthetised 7-week-old mice was gently grasped and lifted using a forceps. A 25-gauge needle (25G 5/8, BDMicro-Fine; Becton Dickinson), bevel side up, was inserted just under the nipple, taking special care not to push the needle into the abdominal cavity. Upon release of the gland, a single-cell suspension of 10⁵ cells/10 μ l of PBS was slowly injected into the mammary fat pad.

A mastectomy was conducted on isoflurane-anaesthetised mice in which the orthotopic tumours were separated from adherent tissues using forceps and excised and stored for further analysis. When during a

mastectomy positive lymph nodes were detected using bioluminescent imaging (BLI), these were also surgically resected. When no detectable residual tumour was found, the surgical incision was closed with stainless steel autoclips.

In the group with large tumours (10⁸ photons/s), three mice were excluded from the group as significant weight loss was observed before they reached the criteria of a large tumour (10⁸ photons/s).

T β RI inhibitor treatment

Mice were treated with vehicle (1% methylcellulose) or SD-208 (60 mg/kg once daily) by oral gavage [15]. No adverse effects of SD-208 on mouse health were detected during the study (Supplementary Figure 1).

Whole-body bioluminescent imaging (BLI)

Tumour growth was monitored by whole-body BLI using an intensified-charge-coupled device (I-CCD) video camera of the *in vivo* Imaging System (IVIS100; Xenogen/Perkin Elmer, Alameda, CA, USA) as described previously [22]. In the SD-208 experimental treatment experiment, the newer IVIS Lumina II (Xenogen/Perkin Elmer) was used for BLI measurements. Mice were anaesthetised using isoflurane and injected i.p. with 2 mg of D-luciferin (Perbio Science Nederland BV, Etten-Leur, The Netherlands). Analyses for each metastatic site were performed after definition of the region of interest and quantified with Living Image 4.2 (Caliper Life Sciences, Teralfene, Belgium). Values are expressed as relative light units (RLU) in photons/s.

Immunofluorescence

Immunofluorescent staining was performed as described previously [24]. In brief, fixed paraffin-embedded tissues were sectioned at 5 μ m. For antigen retrieval, sections were boiled in antigen unmasking solution (Vector Laboratories, Peterborough, UK) and incubated in 3% H₂O₂ for endogenous peroxidase sequestering. The primary antibodies and dilutions used were as follows: rabbit polyclonal α -cleaved caspase-3, 1 : 500 (Cell Signaling Technologies, Danvers, MA, USA; #9661S); rat monoclonal α -CK-8, 1 : 200 (TROMA-I; University of Iowa, Iowa City, IA, USA); rabbit polyclonal α -phospho-histone H3, 1 : 500 (Ser10; Merck Millipore, Amsterdam, The Netherlands); and rabbit monoclonal α -phospho-SMAD2, 1 : 1000 (Ser465/467, 138D4; Cell Signaling). Sections were blocked with 1% bovine serum albumin (BSA)–PBS–0.1% v/v Tween 20 and incubated with primary antibodies diluted in the blocking solution, overnight at 4 °C or room temperature. Sections were then incubated with secondary antibodies labelled with Alexa Fluor 488, 555, or 647 (1 : 250 in PBS–0.1% Tween; Life Technologies/Molecular Probes). The detection of pSMAD2 was enhanced using tyramide amplification (Invitrogen/Molecular Probes) by incubation of the slides with horseradish peroxidase

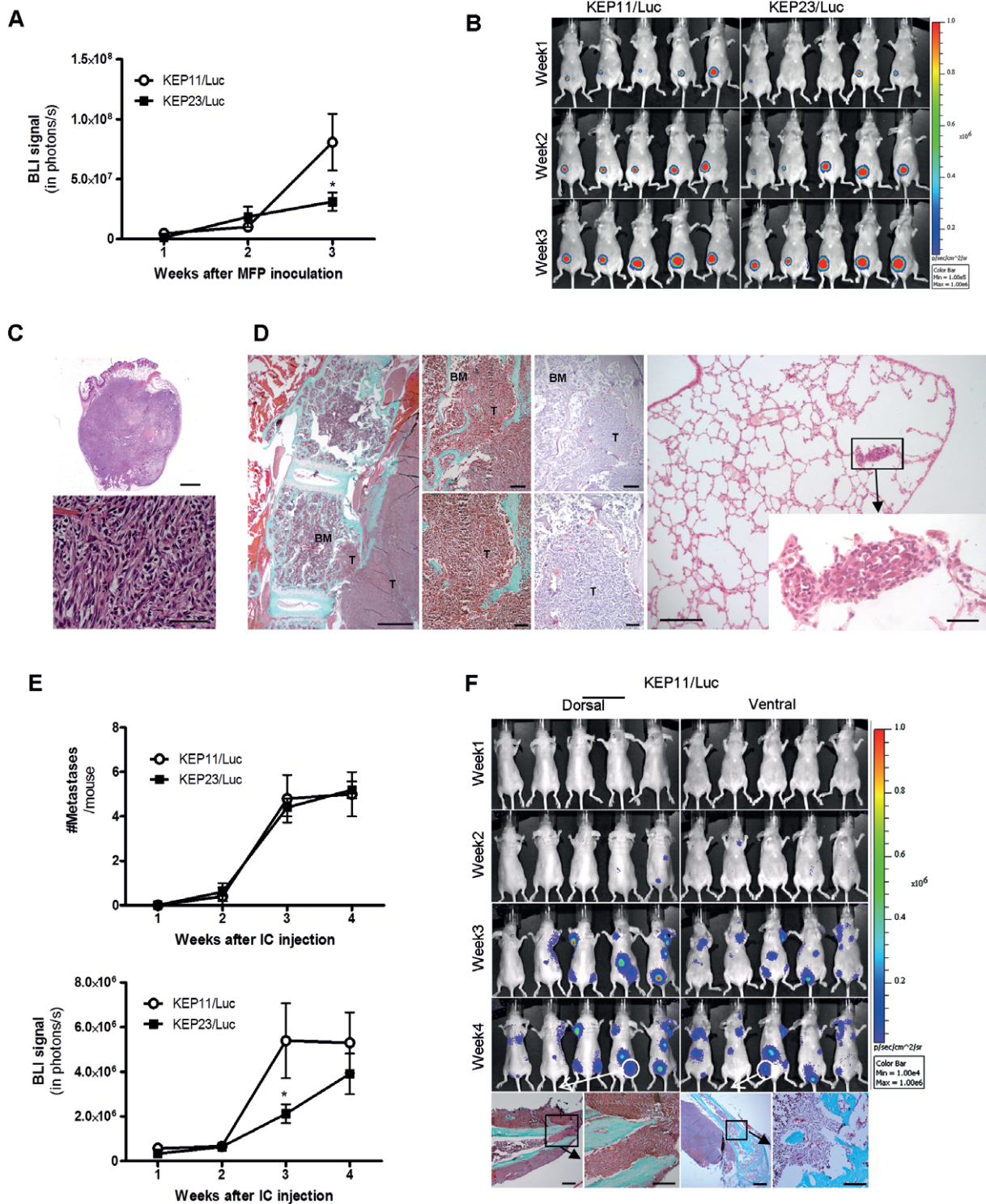


Figure 1. Tumour growth and metastasis of murine ILC cells allografted in immunodeficient mice. Two firefly luciferase-expressing clones, KEP11/Luc and KEP23/Luc, were tested for their ability to grow in athymic nude mice. Both cell lines were orthotopically (A–D) inoculated in the fourth mammary fat pad and in the left cardiac ventricle (E, F) as a preclinical *in vivo* model of bone metastasis. (B, F) Representative examples of whole-body bioluminescent imaging. (C) H&E staining shows that KEP11/Luc tumour cells are characterized by a trabecular or 'single file' arrangement of cells, are poorly differentiated, are small in size, and have pleiomorphic nuclei and spare cytoplasm. Goldner staining of bone sections showed that metastases were mainly present in the axial and appendicular skeleton, including vertebrae (D), tibiae (F, bottom left), and pelvis (F, bottom right). (G) Representative BLI images of KEP11/Luc cells that were inoculated into right tibiae (H, right images) with the contra-lateral tibiae as sham-operated controls (H, left images). (H) X-ray and μ CT images showed that the KEP11/Luc tumours in bone represent a mixed bone phenotype, with both osteolytic and osteo-inductive lesions in close proximity of the tumour. Tumour-induced osteoclastic resorption at the cancellous (upper panels) and cortical (lower panels) bone. Arrows indicate TRAcP⁺ multinucleated osteoclasts. Scale bars: (C) upper figure, 500 μ m; lower figure, 50 μ m; (D) left figure, 500 μ m; upper two panels, 80 μ m; lower two panels, 80 μ m; (F) 100 μ m; magnified image: 20 μ m; (H) all scalebars 40 μ m.

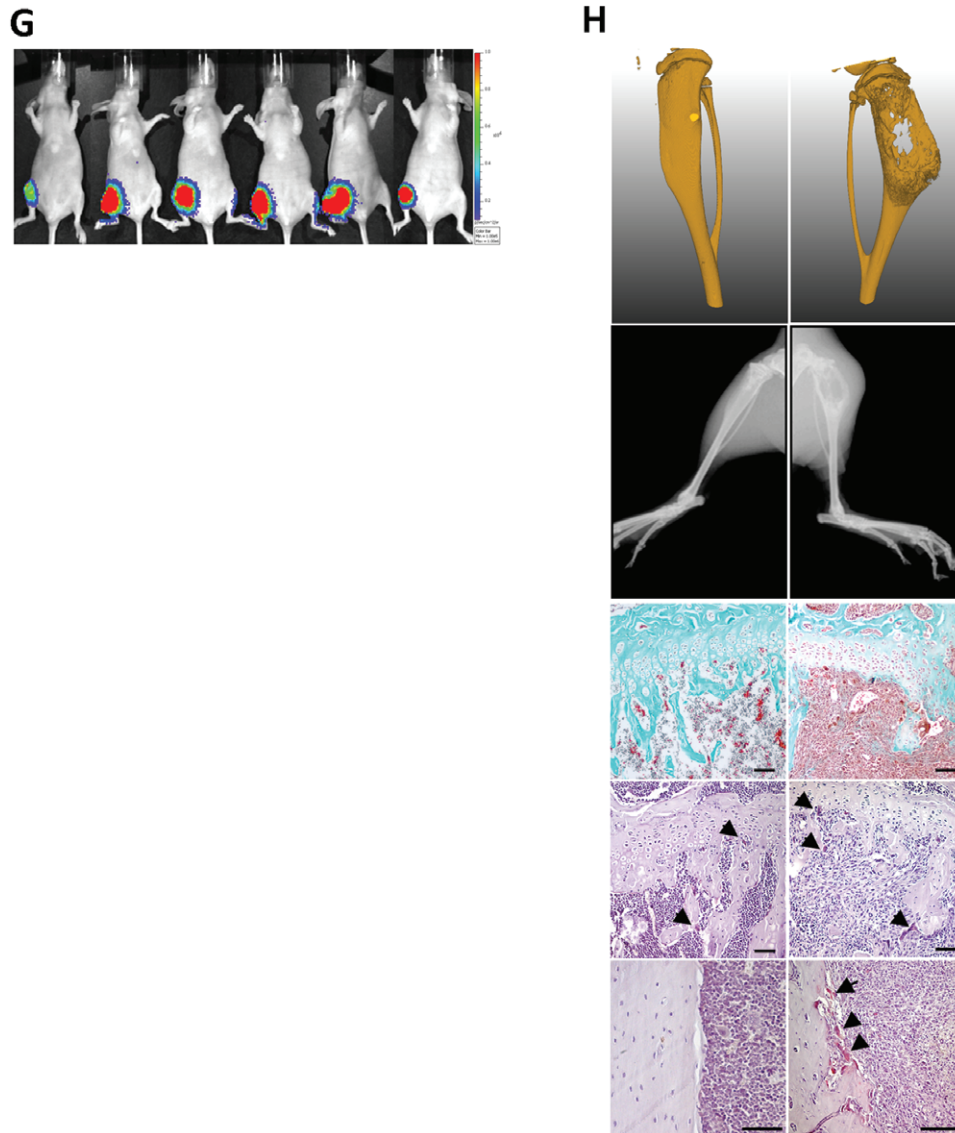


Figure 1. Continued

(HRP)-conjugated secondary antibody (1 : 100 dilution) (Life Technologies/Molecular Probes), followed by incubation with Alexa Fluor 488 tyramide (Life Technologies/Molecular Probes) for 10 min. Nuclei were visualized by TO-PRO3 (1 : 1000 diluted in PBS–0.1% Tween 20; Life Technologies/Molecular Probes) or DAPI, which was included in the mounting medium (Prolong G, Life Technologies/Molecular Probes).

Statistical analysis

Statistical analysis was performed with GraphPad Prism 6.0 software (GraphPad Software Inc, San Diego, CA, USA) with the use of an unpaired Student's *t*-test (for comparison between two groups), a one-way ANOVA with Tukey's multiple comparison test or a two-way ANOVA with Bonferroni's multiple comparison test as stated in the figure legends. All *in vitro* experiments were performed at least three times. Unless stated otherwise, data are represented as mean \pm SEM. *p* values less

than 0.05 were regarded as being statistically significant (**p* < 0.05, ***p* < 0.01, and ****p* < 0.001).

Results

Orthotopic, intracardiac, and intra-osseous models

In order to develop novel preclinical models for ILC, KEP cells were tested in three different *in vivo* models, namely orthotopic, intracardiac, and intra-osseous inoculation models. Orthotopic inoculation of athymic nude mice with either KEP11/Luc or KEP23/Luc cells resulted in 100% tumour take rate (Figures 1A and 1B). Based on BLI measurements, the orthotopic growth of KEP11/Luc was significantly higher than that of KEP23/Luc (Figures 1A and 1B). KEP tumour cells were small in size, had pleiomorphic nuclei, coarsely clumped chromatin, and spare cytoplasm (Figure 1C). In addition, KEP cells were CK8-positive, occasionally

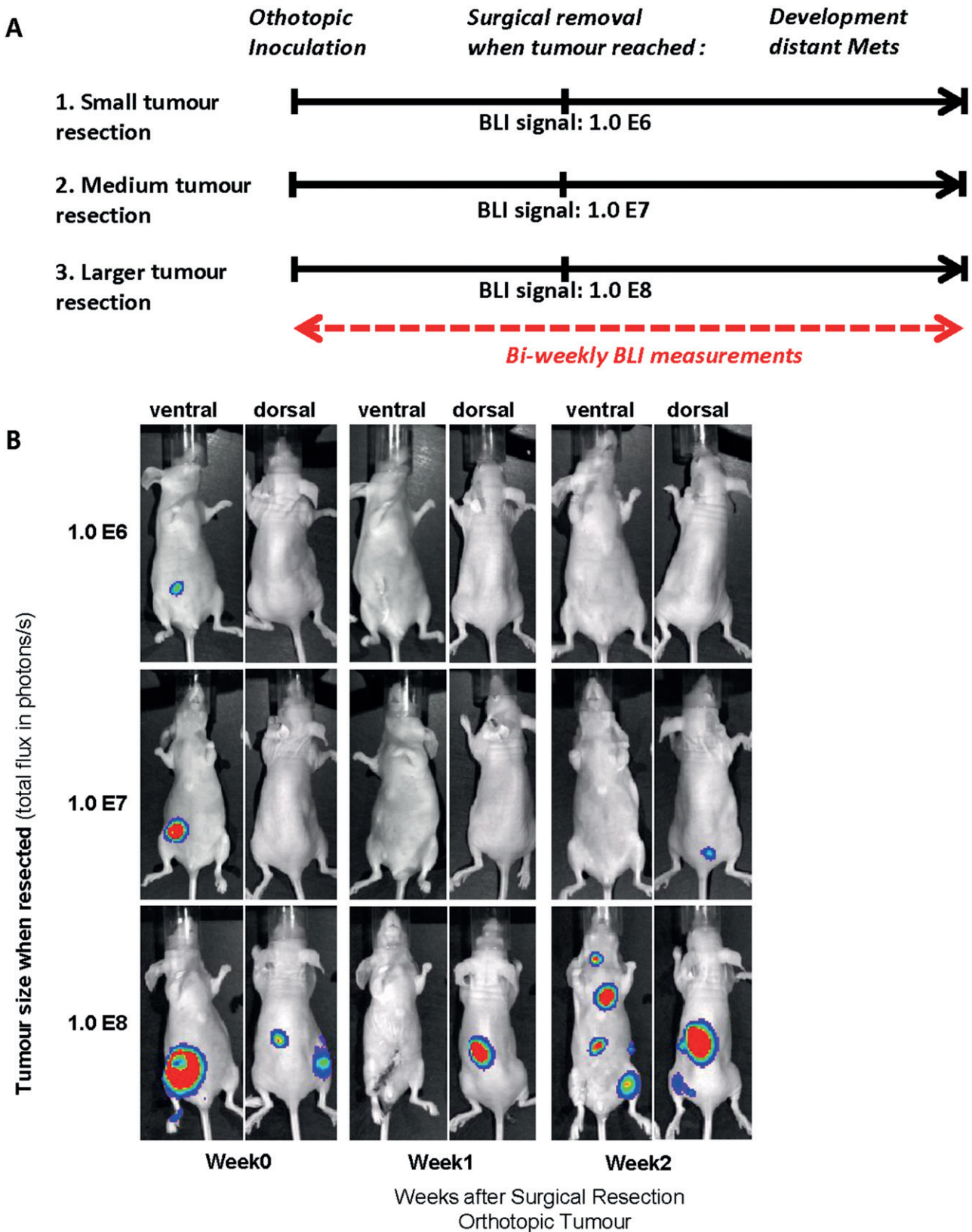


Figure 2. The efficacy of distant metastasis formation after surgical removal of orthotopically implanted murine ILC cells is dependent on the tumour size in the mammary gland. (A) Schematic representation of experimental set-up. 100 000 KEP11/Luc cells were inoculated into fourth mammary fat pad. Mice were divided into three groups ($N = 15$) and orthotopic tumours were surgically resected only when the total BLI signal of the tumour reached ' 10^6 photons/(s · cm² · sr)', ' 10^7 photons/(s · cm² · sr)' or ' 10^8 photons/(s · cm² · sr)'; representative example are shown in B. The number (C) and total size (D) of the distant metastases formed were significantly increased when larger (1E8 versus 1E6 photons/s) orthotopic tumours were resected. * $p < 0.05$, ** $p < 0.01$, and *** $p < 0.001$ versus 1E6, using two-way ANOVA with Bonferroni's multiple comparison test.

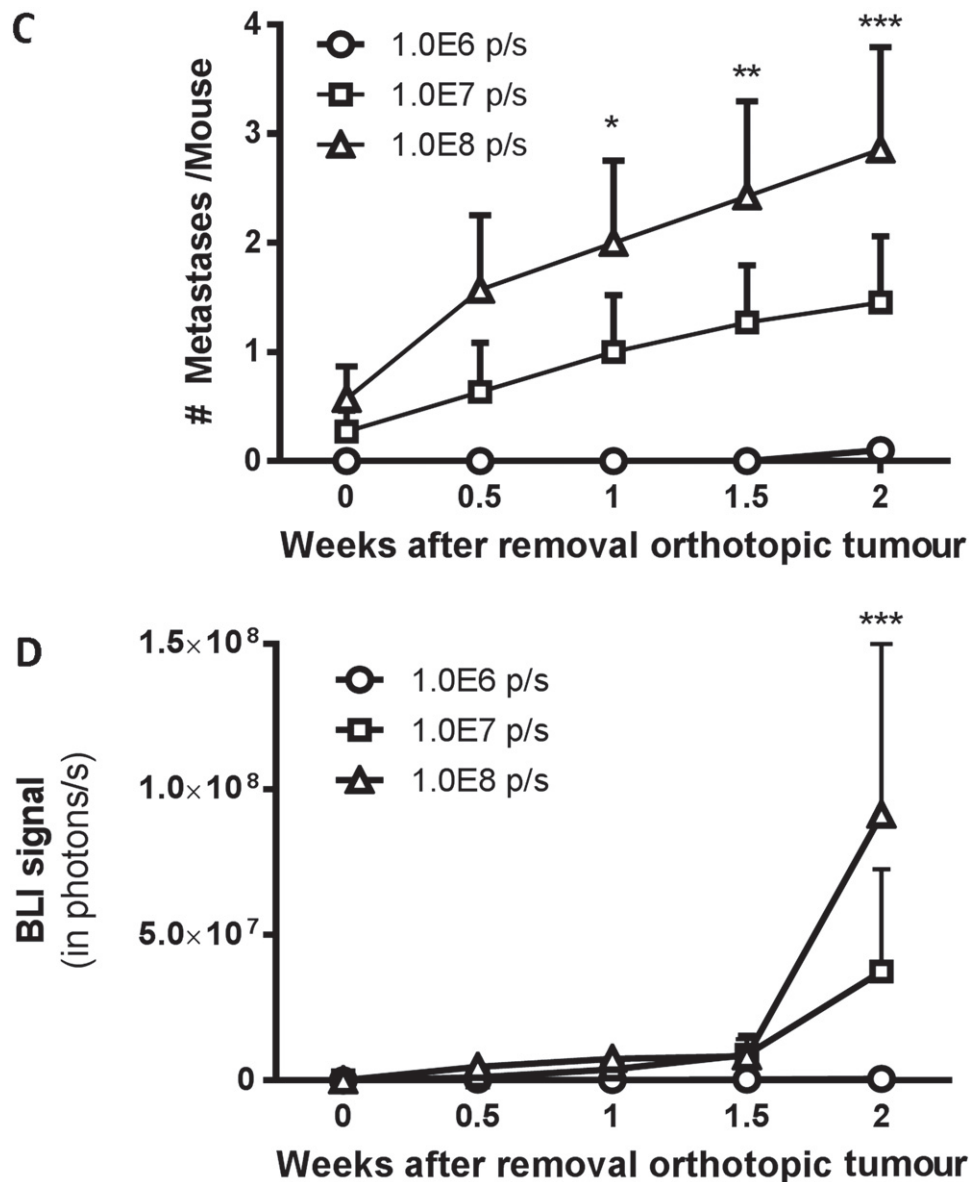


Figure 2. continued

expressed CK14, and did not express SMA (Supplementary Figure 2). After surgical removal of orthotopically implanted tumours, mice appeared tumour-free, as assessed with BLI imaging. Within 3 weeks, however, the formation of distant bone metastases was observed in the axial and appendicular skeleton, including vertebral and tibial metastases (Figure 1C). It is important to note that no overt lung metastases were detected 5 weeks after resection of the orthotopic tumour using BLI. Histological analysis confirmed minimal lung involvement, showing that only 10% (1/10) presented with a micrometastasis (Figure 1C).

Inoculation of KEP11/Luc and KEP23/Luc cells into the left cardiac ventricle led to the rapid development of bone metastases with a comparable distribution pattern and 100% distant tumour take rate (Figures 1D and 1E and Supplementary Figure 3). To further test the ability of KEP cells to grow in the bone marrow microenvironment, tumour cells were injected

in the tibiae. Again, the tumour take rate was 100% (Figure 1F), and the bone phenotype was found to be mixed, with destruction of both cortical bone and ectopic bone formation as shown on 3D μ CT images and histological sections (Figure 1G).

Next, we further refined the orthotopic model by resecting orthotopic tumours of three different sizes ($N=10$) based on BLI signal intensity: namely, small-sized tumour [10^6 photons/(s \cdot cm² \cdot sr)]; medium-sized tumour [10^7 photons/(s \cdot cm² \cdot sr)]; and large-sized tumour [10^8 photons/(s \cdot cm² \cdot sr)].

At the time (corresponding to 12 ± 0 days after orthotopic injection) that small tumours were resected, no distant metastases were present. In the following 2 weeks, only 10% (1/10) of the mice developed a distant metastasis (Figures 2C and 2D). Moreover, no additional metastases developed in the following 3 weeks (data not shown). When medium orthotopic tumours were resected (corresponding to 25 ± 2 days after orthotopic

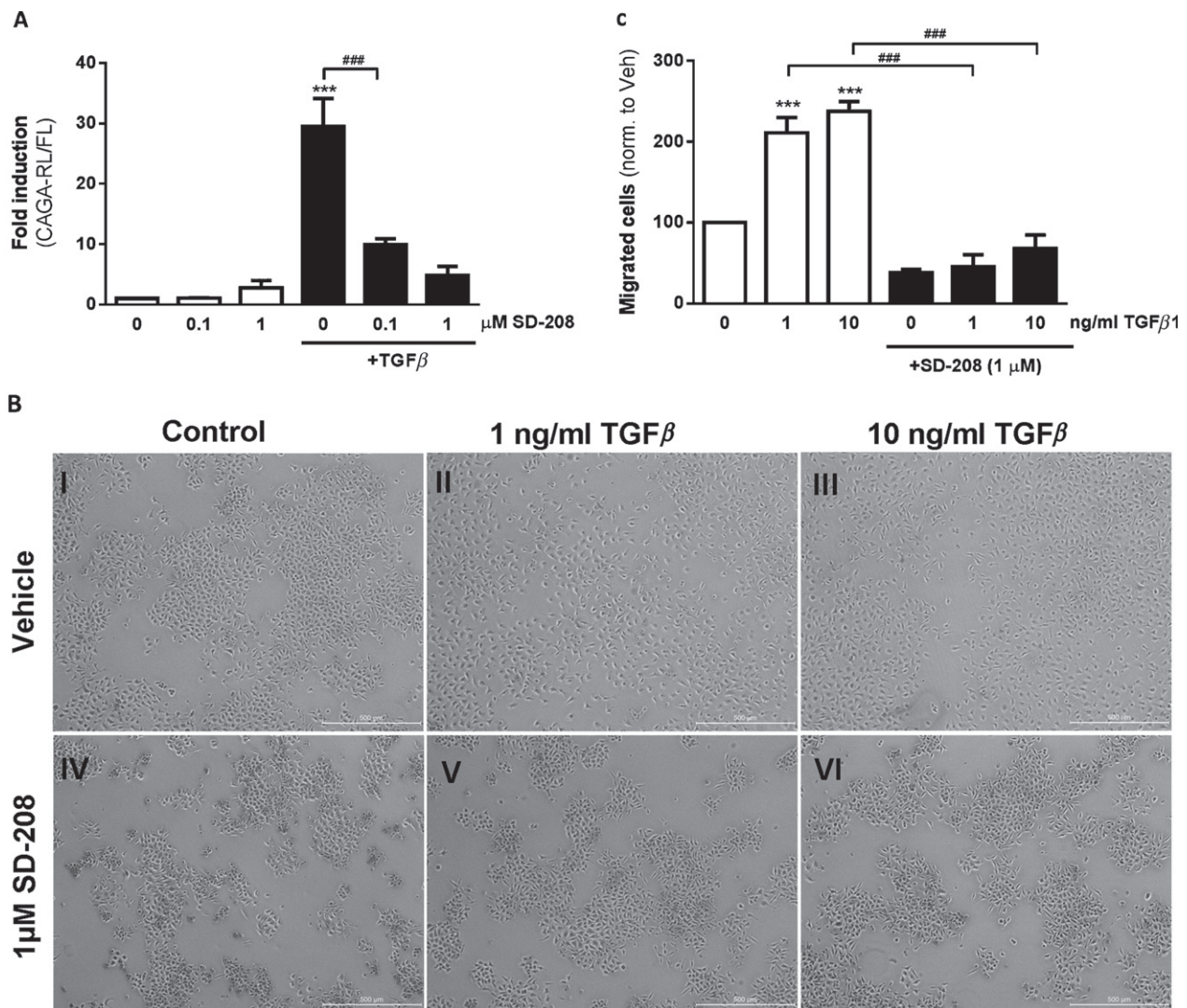


Figure 3. Differential effects of TGFβ on migration, apoptosis, and proliferation *in vitro*. (A) KEP11/firefly luciferase (FL) (KEP11/Luc) cells were transiently transfected with the Smad-dependent TGFβ reporter construct CAGA coupled to *Renilla* luciferase (RL). 5 ng/ml TGFβ1 was used. The average of three independent experiments is shown. *** $p < 0.001$ versus vehicle; ### $p < 0.001$ using one-way ANOVA with Tukey's multiple comparison test. (B) In 2D culture, in unstimulated conditions, KEP cells grow in clumps. Forty-eight hours of TGFβ1 stimulation results in single cell morphology. Co-treatment with 1 μM SD-208 completely blocks the TGFβ effect. (C) Migration assay. The average of three independent experiments is shown. *** $p < 0.05$ versus vehicle; ### $p < 0.05$, using one-way ANOVA with Tukey's multiple comparison test. Effects of TGFβ and SD-208 on viability (D) and apoptosis (E) using the Apo-Tox Glo triple assay. The averages of three independent experiments are shown. * $p < 0.05$ versus vehicle, using two-way ANOVA with Bonferroni's multiple comparison test.

injection), 20% (2/10) of the mice had already presented with at least one distant metastasis. In the following 2 weeks, 60% (6/10) of the mice developed distant metastases (Figures 2C and 2D). When larger-sized tumours were resected (corresponding to 39 ± 2 days after orthotopic injection), 43% (3/7) of the mice had already developed detectable distant metastases at the time of surgery. In the 2 weeks after surgery, 86% (6/7) of the mice had developed at least one distant metastasis (Figures 2C and 2D).

TGFβ stimulates Smad-dependent signalling in KEP cells

To test the ability of the tumour cells to respond to TGFβ1 administration, we transiently transfected the KEP11/firefly-luciferase clone with a Smad-dependent

TGFβ-reporter construct CAGA linked to *Renilla* luciferase (RL). Stimulation with 5 ng/ml TGFβ1 for 24 h resulted in a strong increase (29.5×) in the activity of the CAGA reporter. The TβRI kinase inhibitor SD-208 partially blocked TGFβ-induced signalling at a concentration of 0.1 μM (66% inhibition, $p < 0.05$) and almost completely blocked TGFβ-induced signalling at a concentration of 1 μM (84% inhibition, $p < 0.001$) (Figure 3A).

TGFβ treatment affects cellular morphology and migration

Our *in vitro* data show that treatment with both SD-208 and TGFβ1 exerts morphological changes in tumour cells. While SD-208-treated cells displayed a cuboidal shape and grew in clusters (Figure 3B, IV), cells treated

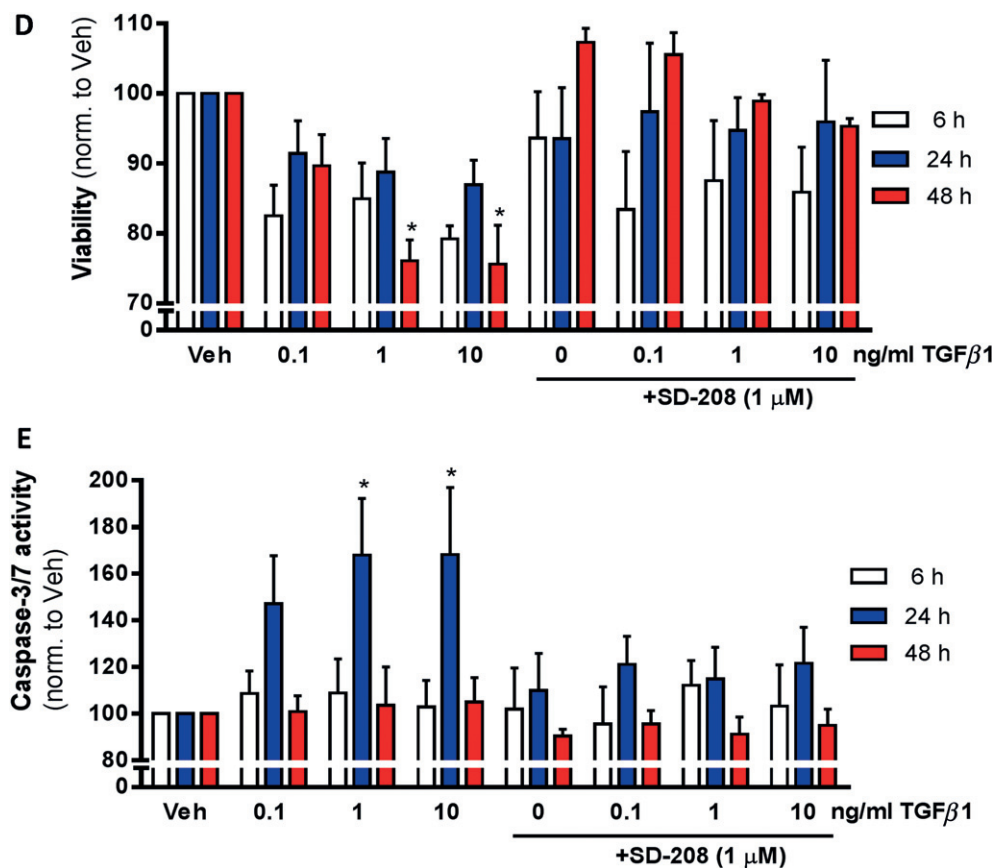


Figure 3. Continued

with TGF β displayed elongated, mesenchymal-like cellular shapes and were more dispersed (Figure 3B, II and III). Co-incubation of TGF β with SD-208 reversed these TGF β -induced changes in morphology towards a more sessile, epithelial-like phenotype (Figure 3B, V and VI). Furthermore, we found that TGF β 1 induced a dose-dependent increase in the migration of the cancer cells. Again, the pro-invasive TGF β 1 response was attenuated upon addition of SD-208 (Figure 3C).

TGF β decreases cellular viability via induction of apoptosis and G1/G0 cell cycle arrest

After 48 h, TGF β 1 (1 and 10 ng/ml) decreased the number of viable cells. This decrease was completely reversed upon co-incubation with SD-208 (Figure 3D). Next, we studied whether induction of apoptosis or inhibition of proliferation accounts for the observation that TGF β treatment resulted in reduced numbers of KEP cells.

As assessed by a caspase-3/7 activity assay, addition of 1 and 10 ng/ml TGF β 1 for 24 h significantly induced apoptosis by 68.0% and 68.2%, respectively (Figure 3E). No significant induction of apoptosis was observed when cells were co-incubated with SD-208.

Next, it was tested whether TGF β 1 treatment also reduced the number of viable cells by inhibiting proliferation via G0/G1 arrest. Treatment of the cells with 10 ng/ml TGF β for 24 and 48 h showed a

significant increase in the G0/G1-phase of the cell cycle. Co-incubation with SD-208 was also able to completely block the TGF β 1-induced increase in the G0/G1-phase (Figures 4A and 4B). Furthermore, treatment with SD-208 alone for 24 h decreased the percentage of cells in the G0/G1-phase significantly ($p < 0.05$), along with a significant increase in the S-phase (Supplementary Figure 4).

To test the role of TGF β signalling in our MRD model of lobular carcinoma of the breast, we treated mice daily with 60 mg/kg SD-208 in a continuous or adjuvant setting (Figure 5A). Based on the data described in Figure 2 and the practical need to have a fixed time point, we chose 4 weeks as the time point for surgical resection after orthotopic inoculation of KEP11/Luc cells. Continuous treatment with SD-208 for 4 weeks of orthotopically implanted tumour cells resulted in significantly increased tumour growth in the mammary glands (Figure 5B). In addition, continuous SD-208 treatment resulted in a significant increase of the number of distant metastases 4 weeks after surgical removal and a clear trend for increased metastatic tumour burden (Figure 5C). Adjuvant SD-208 treatment, which was started after surgical resection of the tumour, also resulted in a significant increase in the number of distant metastases 5 weeks after surgical removal (Figure 5C). Immunolocalisation of phosphorylated Smad2 as a marker for Smad-dependent TGF β signalling confirmed that both tumour cells and

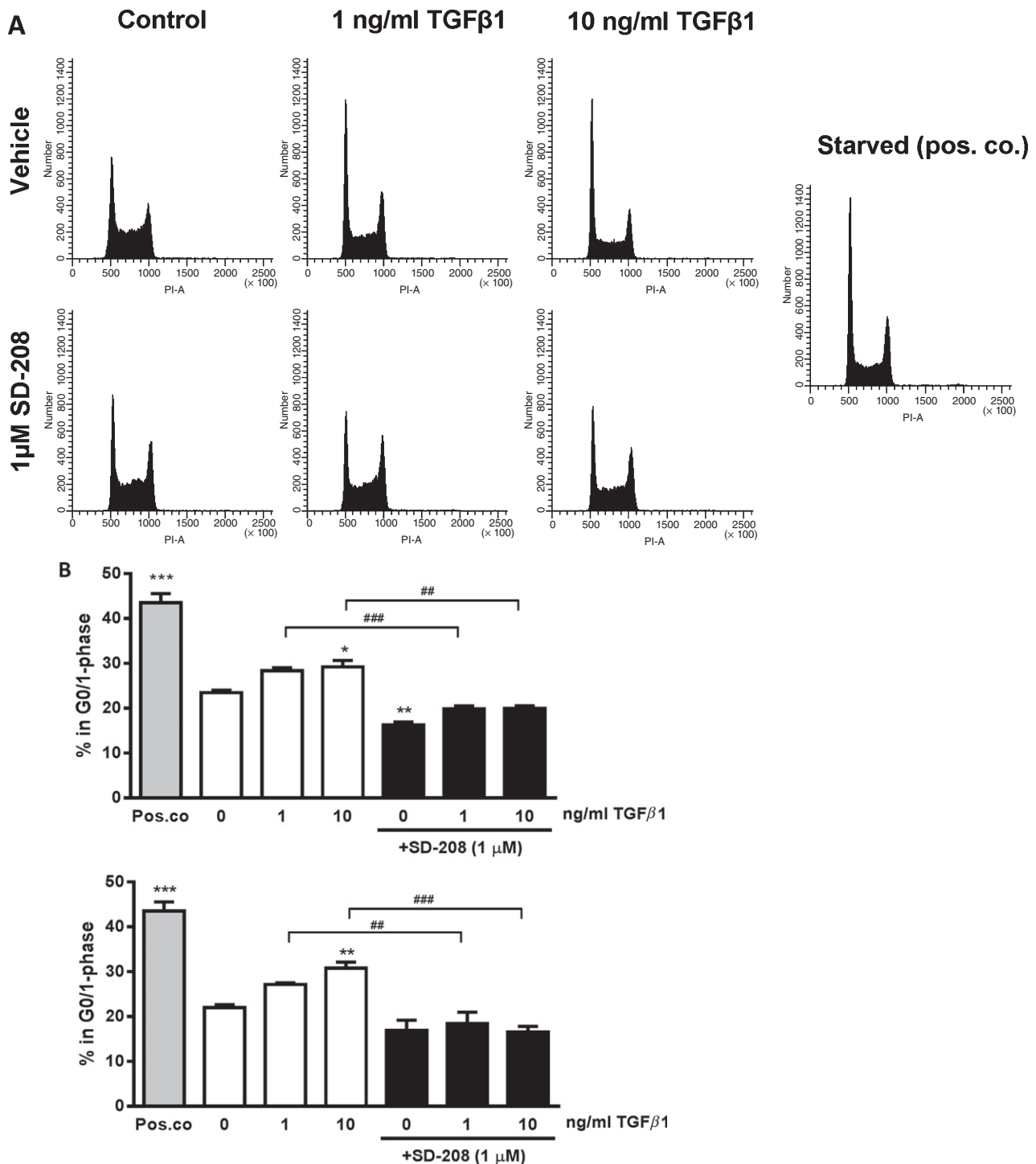


Figure 4. SD-208 blocks TGF β -induced G0/1 arrest in murine ILC cells. (A) Representative examples of propidium iodide staining 48 h after stimulation using flow cytometry. (B) SD-208 blocks TGF β -induced G0/1 arrest at 24 (upper graph) and 48 h (lower graph). The average of three independent experiments is shown. * $p < 0.05$ versus vehicle, ** $p < 0.01$ versus vehicle; ## $p < 0.01$; ### $p < 0.001$, using one-way ANOVA with Tukey's multiple comparison test.

the tumour-associated stromal cells display reduced TGF β signalling upon SD-208 treatment at orthotopic sites (Figure 6A). In line with our *in vitro* findings (Figure 3B), SD-208 treatment resulted in cancer cells that displayed a more epithelial-like phenotype *in vivo* (Figure 6A).

Immunolocalisation of phospho-histone H3-positive and cleaved caspase-3-positive cells *in vivo* revealed

proliferating and apoptotic cells, respectively. Most apoptotic cells were detected in the central part of the tumour. In the periphery of the tumour, SD-208 treatment decreased the number of apoptotic cells by 73% (from 36.7 to 9.9 cells/mm², $p < 0.05$; Figure 6B), while the number of apoptotic cells were reduced by 94% in the core region of the tumour (from 129.2 to 7.3 cells/mm², $p < 0.05$; Figure 6B). While the 61%

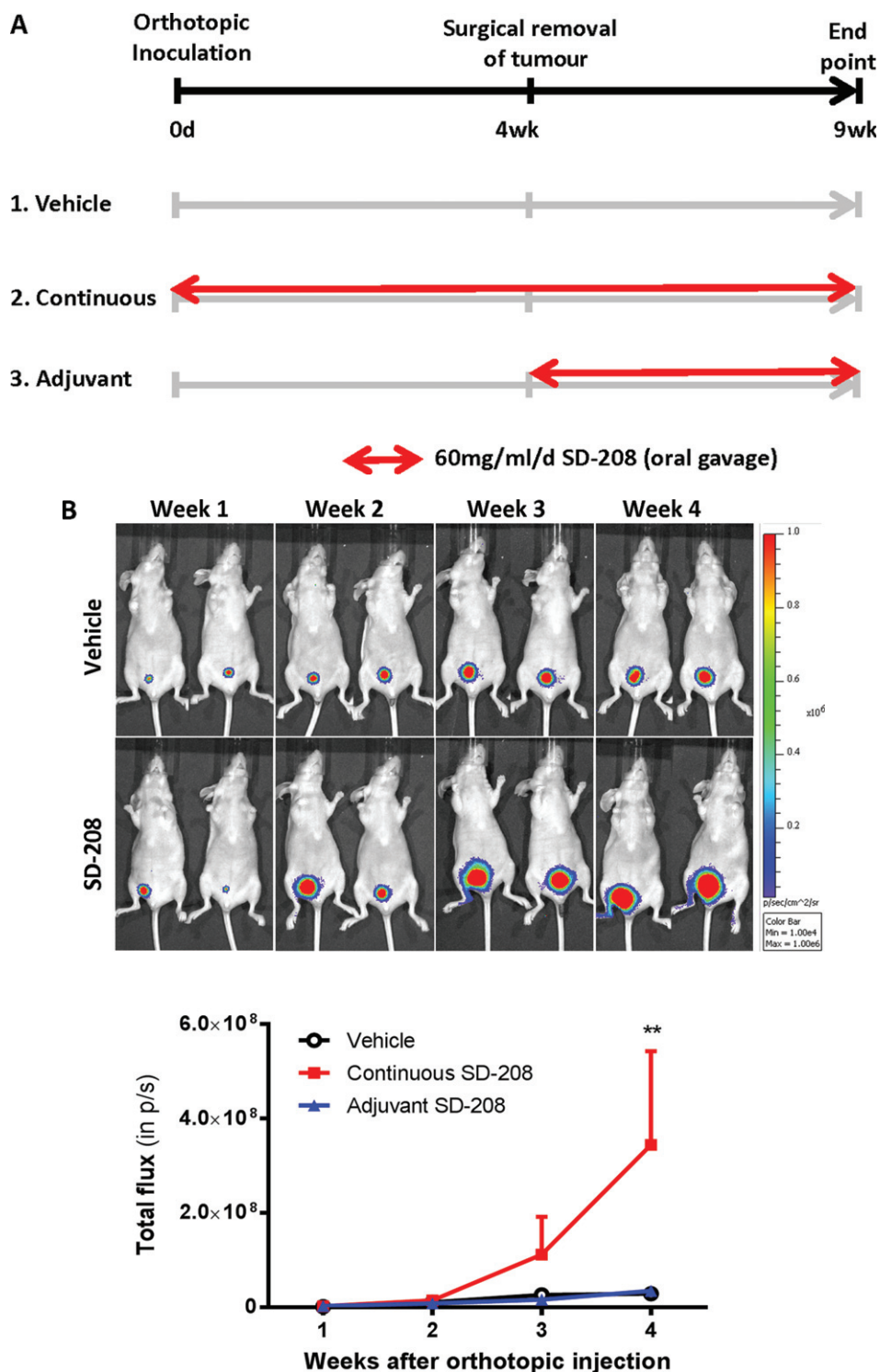


Figure 5. SD-208 treatment increases orthotopic tumour growth and the formation of distant metastases. (A) Schematic representation of the experimental set-up ($N = 15$). (B) SD-208 stimulates the orthotopic growth of KEP11/Luc tumour cells. (C) The formation of distant metastases is increased upon SD-208 treatment. * $p < 0.05$ versus vehicle; ** $p < 0.01$ versus vehicle, using two-way ANOVA with Bonferroni's multiple comparison test.

increase (from 12.8 to 20.5 cells/mm², $p < 0.001$) in the number of proliferating cells upon SD-208 treatment in the central region did not reach statistical significance, SD-208 treatment significantly increased the number of proliferating cells by 121% (from 24.7 to 55.2 cells/mm², $p < 0.001$) in the periphery of the tumour (Figure 6C).

Discussion

We have developed a novel mouse model of MRD for invasive lobular breast cancer that recapitulates the key events of the metastatic cascade. Using whole-body BLI, we performed cancer cell tracking and therapy response in real time. We mimicked the clinical setting

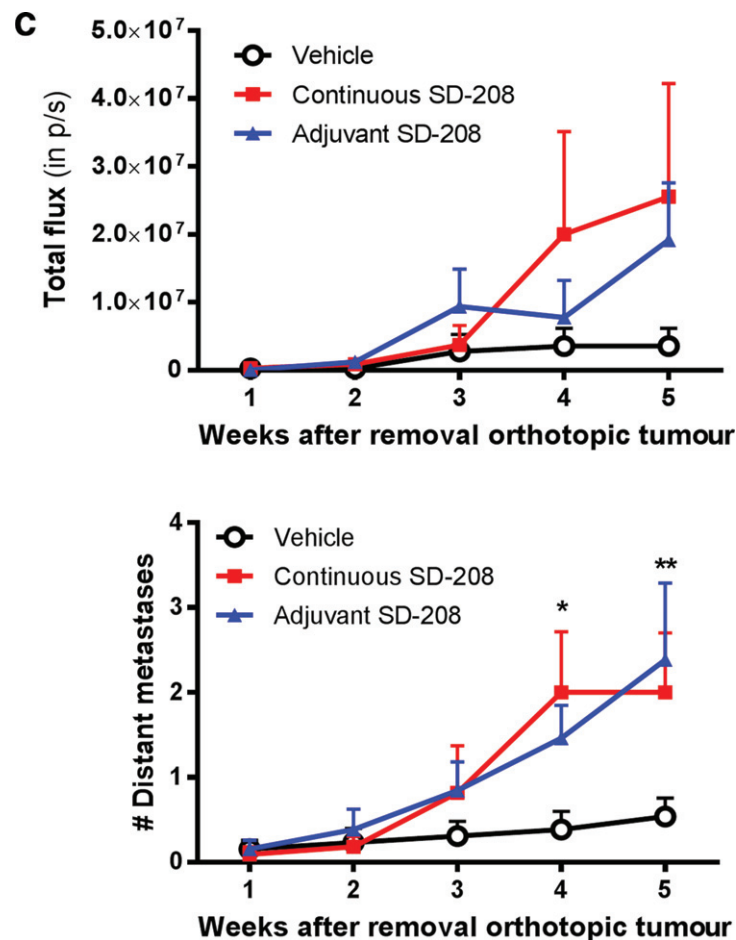


Figure 5. Continued

by surgical resection of orthotopic tumours to extend the life span of the animals, thus allowing disseminated cancer cells to develop into overt metastases. As a result, mice eventually succumbed to widespread metastatic bone disease without overt lung metastases that hamper the life span of the animals. Our model provides a valuable tool to study dissemination to bone of ILC and offers several advantages over most of the currently available metastasis models.

Metastasis formation in our model is not induced by systemic (intravenous, intracardiac) injection of cancer cells, but occurs spontaneously from the orthotopic site. Thus, metastatic dissemination in this model more closely reflects the initial key biological events of the metastatic cascade. While in most other orthotopic breast cancer models bone metastases are not observed, our preclinical model includes mainly skeletal metastases with minimal lung involvement. This seems to be a major advantage over the murine 4 T1 model [7–9]. Furthermore, BLI allows sensitive non-invasive monitoring of orthotopic tumour growth and metastasis in real time. This model seems to be ideally suited for testing novel therapeutic agents and treatment protocols aiming at preventing or treating metastatic disease. As shown by our intervention experiments, this can be performed in either an adjuvant or a neoadjuvant setting, thus allowing a careful and independent

evaluation of therapeutic agents targeting the primary tumour, dissemination of tumour cells, and/or metastatic bone disease. In the model described here, BLI comes at the expense of an immune-proficient microenvironment because luciferase-expressing tumour cells might provoke a specific immune response to luciferase [25]. Without the use of *in vivo* non-invasive imaging markers, Doornebal *et al* elegantly showed that serial transplantation of fragments of KEP tumours also resulted in the formation of distant metastases from orthotopic sites in a syngeneic model, although the involvement of metastasis to bone was not explicitly mentioned [26].

It has been well documented that TGF β has a dual role in cancer development. While the anti-tumourigenic effects are generally most prominent during the initial steps of carcinogenesis, pro-tumourigenic effects may prevail at later stages [11,27]. While the net effect of TGF β in several mouse models of IDC is clearly pro-tumourigenic, the anti-tumour effects of TGF β predominate in our ILC mouse model through stimulation of apoptosis and induction of a G0/1 arrest.

Although not dominating the overall effect, pro-tumourigenic effects on migration may also occur *in vivo*. The number of metastases formed after resection of the orthotopic tumour was comparable in mice treated continuously or in the adjuvant setting. However, the orthotopic tumours that were resected were bigger in the

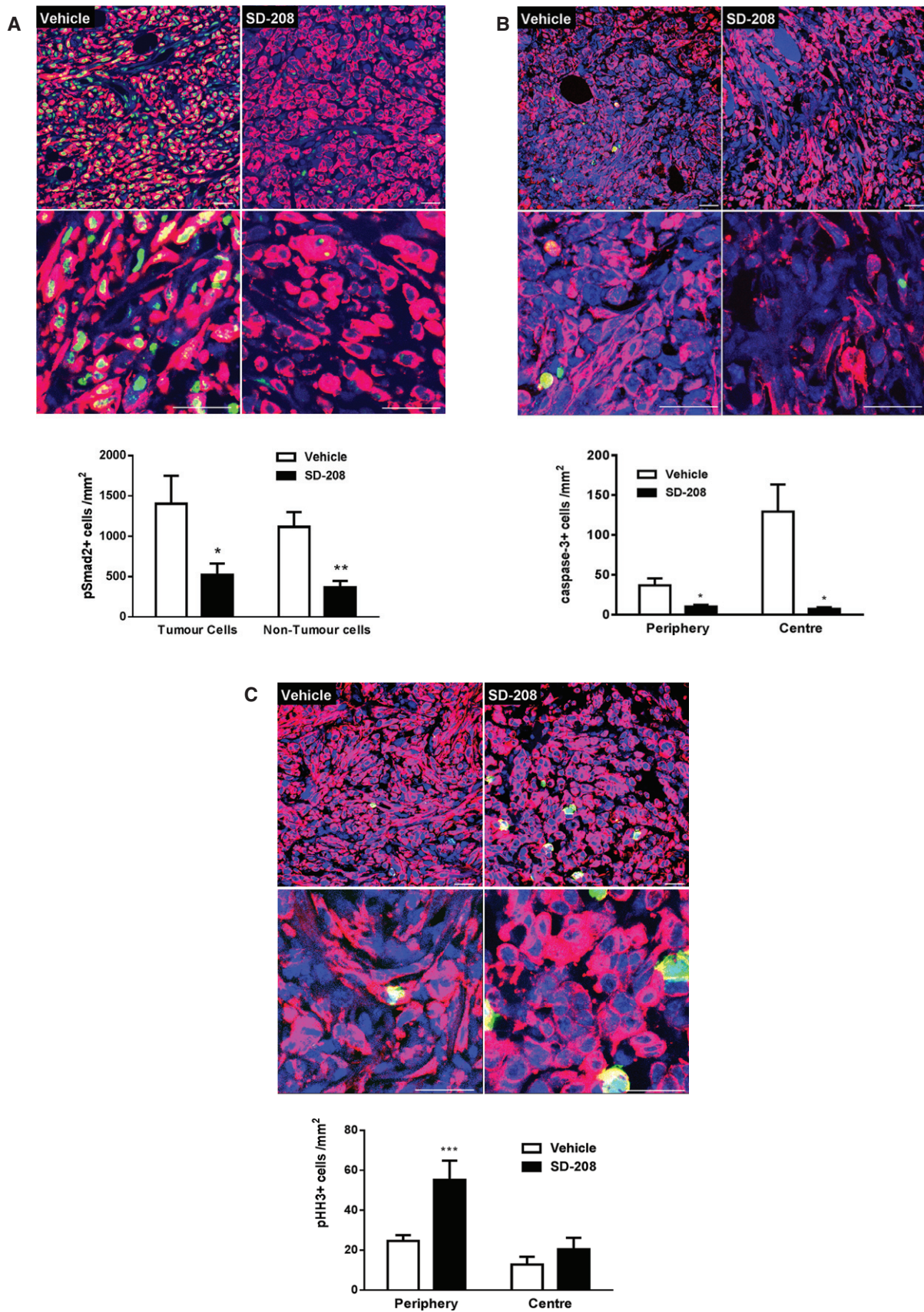


Figure 6. Effects of SD-208 on TGFβ signalling, apoptosis, and proliferation in orthotopic tumours by immunofluorescence. Nuclei were visualized with DAPI (blue) and cytokeratin-8-positive tumour cells are represented in red. Phospho-Smad2 for detection of active Smad-dependent TGFβ signalling (A), cleaved caspase-3 for detection of apoptotic cells (B), and phospho-histone H3 for detection of proliferating cells (C) are represented in green. Yellow represents an overlay of green and red colours. SD-208 treatment decreased TGFβ signalling in both CK8-positive (tumour cells) and CK8-negative (non-tumour) cells. **p* < 0.05 versus vehicle; ***p* < 0.01 versus vehicle; ****p* < 0.001 versus vehicle, using an unpaired Student's *t*-test. All scale bars = 25 μm.

mice that were treated continuously versus those in an adjuvant setting (no SD-208 before surgical resection). Despite SD-208-induced stimulation of orthotopic tumour growth, SD-208 may therefore still display its (less prominent) anti-invasive properties.

While SD-208 increased tumour growth in our model, many studies have shown that TGF β blockade decreased tumour progression and metastasis in mouse models of IDC [17,28–30]. Using 4 T1 and MDA-MB-231 IDC cells, Liu *et al* recently reported that TGF β blockade not only inhibited orthotopic tumour growth, but also improved the penetration of chemotherapeutic drugs by normalization of the intratumoural vascularization and decreasing collagen I production [29]. Although pharmacological blockade of the TGF β pathway may not diminish tumour growth in our ILC model, it is tempting to speculate that the observed increase in proliferation may even be exploited therapeutically when used in combination with chemotherapeutic agents.

Gene expression profiling studies have suggested that deregulated TGF β signalling is more important in ILC than in IDC [31,32]. However, interpretation of these results is hampered by the fact that the affected gene expression patterns are not consistent in comparable studies using different patient populations and cohorts [31–35]. Based on the high sensitivity to the anti-tumourigenic effects of TGF β in our ILC model, or rather the stimulatory effect on tumour growth upon TGF β signalling blockage, it would be highly interesting to study functionally whether ILC patients are more sensitive to the anti-tumourigenic effects of TGF β than IDC patients. The outcome of these studies may be of help in deciding which group of patients should be included in intervention studies with TGF β blockers.

In conclusion, we developed a novel preclinical orthotopic model of ILC that will lead to spontaneous bone (micro)metastasis with no (significant) lung involvement. In addition, pharmacological treatment with the small molecule SD-208, a T β RI kinase inhibitor, stimulated tumour growth at primary and metastatic sites, indicating that anti-tumour effects prevail in this model.

Acknowledgments

This study was supported by an ITN grant from the European Union's Seventh Framework Programme (FP7/2007-2013, BONE-NET, 264817) and The Netherlands Organization for Scientific Research (NWO, VENI-Grant, 916.131.10).

Author contribution statement

JTB, HC, and MM designed, carried out, and analysed *in vivo* experiments. KMM, JTB, and WEC designed, carried out, and analysed flow cytometry experiments.

KMM, RC, and JTB designed, carried out, and analysed all the other *in vitro* experiments. JTB and MKJ designed, carried out, and analysed immunofluorescent histochemistry. TJS, JTB, and HC designed, carried out, and analysed μ CT experiments. JTB, KSM, JJ, TAG, and GP designed the *in vivo* studies and interpreted the data. JTB, KMM, and GP wrote the manuscript. All authors read, revised, and approved the final manuscript.

Abbreviations

BLI, bioluminescent imaging; EMT, epithelial-to-mesenchymal transition; GEMM, genetically engineered mouse model; IDC, invasive ductal carcinoma; ILC, invasive lobular carcinoma; MRD, minimal residual disease; RLU, relative light unit; T β RI, TGF β receptor I

References

- Li CI, Anderson BO, Daling JR, *et al*. Trends in incidence rates of invasive lobular and ductal breast carcinoma. *J Am Med Assoc* 2003; **289**: 1421–1424.
- Martinez V, Azzopardi JG. Invasive lobular carcinoma of the breast: incidence and variants. *Histopathology* 1979; **3**: 467–488.
- Arpino G, Bardou VJ, Clark GM, *et al*. Infiltrating lobular carcinoma of the breast: tumor characteristics and clinical outcome. *Breast Cancer Res* 2004; **6**: R149–R156.
- Jonkers J, Derksen PW. Modeling metastatic breast cancer in mice. *J Mammary Gland Biol Neoplasia* 2007; **12**: 191–203.
- Fantozzi A, Christofori G. Mouse models of breast cancer metastasis. *Breast Cancer Res* 2006; **8**: 212.
- Francia G, Cruz-Munoz W, Man S, *et al*. Mouse models of advanced spontaneous metastasis for experimental therapeutics. *Nature Rev Cancer* 2011; **11**: 135–141.
- Bolin C, Tawara K, Sutherland C, *et al*. Oncostatin M promotes mammary tumor metastasis to bone and osteolytic bone degradation. *Genes Cancer* 2012; **3**: 117–130.
- Tao K, Fang M, Alroy J, *et al*. Imagable 4 T1 model for the study of late stage breast cancer. *BMC Cancer* 2008; **8**: 228.
- Lelekakis M, Moseley JM, Martin TJ, *et al*. A novel orthotopic model of breast cancer metastasis to bone. *Clin Exp Metastasis* 1999; **17**: 163–170.
- Derksen PW, Liu X, Saridin F, *et al*. Somatic inactivation of E-cadherin and p53 in mice leads to metastatic lobular mammary carcinoma through induction of anoikis resistance and angiogenesis. *Cancer Cell* 2006; **10**: 437–449.
- Massague J. TGF β in cancer. *Cell* 2008; **134**: 215–230.
- Roberts AB, Wakefield LM. The two faces of transforming growth factor beta in carcinogenesis. *Proc Natl Acad Sci U S A* 2003; **100**: 8621–8623.
- Buijs JT, Stayrook KR, Guise TA. The role of TGF-beta in bone metastasis: novel therapeutic perspectives. *Bonekey Rep* 2012; **1**: 96.
- Ge R, Rajeev V, Ray P, *et al*. Inhibition of growth and metastasis of mouse mammary carcinoma by selective inhibitor of transforming growth factor-beta type I receptor kinase *in vivo*. *Clin Cancer Res* 2006; **12**: 4315–4330.
- Mohammad KS, Javelaud D, Fournier PG, *et al*. TGF-beta-RI kinase inhibitor SD-208 reduces the development and progression of melanoma bone metastases. *Cancer Res* 2011; **71**: 175–184.

16. Nam JS, Terabe M, Mamura M, *et al.* An anti-transforming growth factor beta antibody suppresses metastasis via cooperative effects on multiple cell compartments. *Cancer Res* 2008; **68**: 3835–3843.
17. Yin JJ, Selander K, Chirgwin JM, *et al.* TGF-beta signaling blockade inhibits PTHrP secretion by breast cancer cells and bone metastases development. *J Clin Invest* 1999; **103**: 197–206.
18. Akhurst RJ, Hata A. Targeting the TGF β signalling pathway in disease. *Nature Rev Drug Discov* 2012; **11**: 790–811.
19. Dennler S, Itoh S, Vivien D, *et al.* Direct binding of Smad3 and Smad4 to critical TGF beta-inducible elements in the promoter of human plasminogen activator inhibitor-type 1 gene. *EMBO J* 1998; **17**: 3091–3100.
20. Uhl M, Aulwurm S, Wischhusen J, *et al.* SD-208, a novel transforming growth factor beta receptor I kinase inhibitor, inhibits growth and invasiveness and enhances immunogenicity of murine and human glioma cells *in vitro* and *in vivo*. *Cancer Res* 2004; **64**: 7954–7961.
21. Buijs JT, Henriquez NV, van Overveld PG, *et al.* Bone morphogenetic protein 7 in the development and treatment of bone metastases from breast cancer. *Cancer Res* 2007; **67**: 8742–8751.
22. van der Pluijm G, Que I, Sijmons B, *et al.* Interference with the microenvironmental support impairs the *de novo* formation of bone metastases *in vivo*. *Cancer Res* 2005; **65**: 7682–7690.
23. Buijs JT, Que I, Lowik CW, *et al.* Inhibition of bone resorption and growth of breast cancer in the bone microenvironment. *Bone* 2009; **44**: 380–386.
24. Karkampouna S, Kruithof BP, Kloen P, *et al.* Novel *ex vivo* culture method for the study of Dupuytren's disease: effects of TGF β type 1 receptor modulation by antisense oligonucleotides. *Mol Ther Nucleic Acids* 2014; **3**: e142.
25. Jeon YH, Choi Y, Kang JH, *et al.* Immune response to firefly luciferase as a naked DNA. *Cancer Biol Ther* 2007; **6**: 781–786.
26. Doornebal CW, Klarenbeek S, Braumuller TM, *et al.* A preclinical mouse model of invasive lobular breast cancer metastasis. *Cancer Res* 2013; **73**: 353–363.
27. Ikushima H, Miyazono K. TGF β signalling: a complex web in cancer progression. *Nature Rev Cancer* 2010; **10**: 415–424.
28. Ganapathy V, Ge R, Grazioli A, *et al.* Targeting the transforming growth factor-beta pathway inhibits human basal-like breast cancer metastasis. *Mol Cancer* 2010; **9**: 122.
29. Liu J, Liao S, Diop-Frimpong B, *et al.* TGF-beta blockade improves the distribution and efficacy of therapeutics in breast carcinoma by normalizing the tumor stroma. *Proc Natl Acad Sci U S A* 2012; **109**: 16618–16623.
30. Muraoka RS, Dumont N, Ritter CA, *et al.* Blockade of TGF-beta inhibits mammary tumor cell viability, migration, and metastases. *J Clin Invest* 2002; **109**: 1551–1559.
31. Da Silva L, Parry S, Reid L, *et al.* Aberrant expression of E-cadherin in lobular carcinomas of the breast. *Am J Surg Pathol* 2008; **32**: 773–783.
32. Weigelt B, Geyer FC, Natrajan R, *et al.* The molecular underpinning of lobular histological growth pattern: a genome-wide transcriptomic analysis of invasive lobular carcinomas and grade- and molecular subtype-matched invasive ductal carcinomas of no special type. *J Pathol* 2010; **220**: 45–57.
33. Bertucci F, Orsetti B, Negre V, *et al.* Lobular and ductal carcinomas of the breast have distinct genomic and expression profiles. *Oncogene* 2008; **27**: 5359–5372.
34. Korkola JE, DeVries S, Fridlyand J, *et al.* Differentiation of lobular versus ductal breast carcinomas by expression microarray analysis. *Cancer Res* 2003; **63**: 7167–7175.
35. Turashvili G, Bouchal J, Baumforth K, *et al.* Novel markers for differentiation of lobular and ductal invasive breast carcinomas by laser microdissection and microarray analysis. *BMC Cancer* 2007; **7**: 55.

SUPPORTING INFORMATION ON THE INTERNET

The following supporting information may be found in the online version of this article:

Figure S1. Daily treatment with SD-208 does not affect body length or weight of Balb/c *nu/nu* mice.

Figure S2. Characterization of KEP11/Luc orthotopic tumour by immunofluorescence microscopy.

Figure S3. Inoculation of KEP23/Luc cells into the left cardiac ventricle of immunodeficient mice leads to the formation of multiple bone metastases.

Figure S4. SD-208 blocks TGF β -induced G0/I arrest in KEP cells.